

Microstructural, dielectric and ferroelectric properties of calcium-modified lead titanate thin films derived by chemical processes

D.S.L. Pontes^a, E.R. Leite^a, F.M. Pontes^a, E. Longo^a, J.A. Varela^{b,*}

^aDepartment of Chemistry, Federal University of São Carlos-UFSCar, Caixa Postal 676, 13560-905 São Carlos, SP, Brazil

^bInstitute of Chemistry, UNESP, Caixa Postal 355, 14801-970 Araraquara, SP, Brazil

Received 25 May 2000; received in revised form 12 October 2000; accepted 21 October 2000

Abstract

Ferroelectric $Pb_{1-x}Ca_xTiO_3$ ($x=0.24$) thin films were formed on a Pt/Ti/SiO₂/Si substrate by the polymeric precursor method using the dip-coating technique for their deposition. Characterization of the films by X-ray diffraction showed a perovskite single phase with a tetragonal structure after annealing at 700°C. Atomic force microscopy (AFM) analyses showed that the film had a smooth and crack-free surface with low surface roughness. In addition, the PCT thin film had a granular structure with an 80 nm grain size. The thickness of the films observed by the scanning electron microscopy (SEM) is 550 nm and there is a good adhesion between the film and substrate. For the electrical measurements metal-ferroelectric-metal of the type capacitors were obtained, where the thin films showed good dielectric and ferroelectric properties. The dielectric constant and dissipation factor at 1 kHz and measured at room temperature were found to be 457 and 0.03, respectively. The remanent polarization and coercive field for the deposited films were $P_r=17 \mu C/cm^2$ and $E_c=75 kV/cm$, respectively. Moreover, the 550-nm-thick film showed a current density in the order of $10^{-8} A/cm^2$ at the applied voltage of 2 V. The high values of the thin film's dielectric properties are attributed to its excellent microstructural quality and the chemical homogeneity obtained by the polymeric precursor method. © 2001 Elsevier Science Ltd. All rights reserved.

Keywords: Ferroelectric properties; Films; (Pb, Ca)TiO₃; Precursors; Precursors-organic

1. Introduction

Ferroelectric thin films have attracted much attention as a result of their application in piezoelectric and pyroelectric sensors, dynamic random access memories (DRAM) and non-volatile ferroelectric random access memories (NVFRAM).^{1–3} Modified lead titanate (PbTiO₃) thin films have also attracted interest owing to their good ferroelectric properties. Among the modified lead titanate thin films, the zirconate-modified lead titanate (PZT), lanthanum-modified lead titanate (PLT), and lanthanum–zirconate-modified lead titanate (PLZT) thin films have been widely studied.^{4–6} The production of these modified lead titanate thin films, however, presents some problems insofar as the preparation technique is concerned. Stoichiometry is difficult to achieve in physical preparation methods due to the preferential sputtering

of one element over the other and the different vapour pressures of the constituents. On the other hand, chemical methods such as sol-gel processing require the use of precursor solutions, in which compatibility between the starting reagents constitutes the main problem. Thus, the commonly used alkoxide precursors employed in the production of modified lead titanate thin films by sol-gel methods are highly reactive, requiring careful control of the hydrolysis-condensation reactions. Furthermore, handling the methoxyethanol used as a solvent is quite dangerous. The chemical method known as PPM (polymeric precursor method), on the other hand, is a promising candidate to process a variety of thin films including modified lead titanate [7–10]. Because the polymeric precursor method allows for spin- or dip-coating deposition, it offers several advantages over other processing techniques, i.e. it is a simple inexpensive non vacuum chemical process, it can be used to uniformly deposit several polycomponent oxide thin films, and it uses water as the solvent. In this process, the desired metal cations are chelated in a solution using

* Corresponding author. Tel.: +55-16-222-2022; fax: +55-16-222-7932.

E-mail address: varela@iq.unesp.br (J.A. Varela).

a hydroxycarboxylic acid, such as citric acid, as the chelating agent. This solution is then mixed with a poly-hydroxy alcohol such as ethylene glycol and heated to promote esterification reactions in the solution. Metal ions are chelated by the carboxyl groups and remain homogeneously distributed in the polymeric network.

Yamaka et al.¹¹ reported highly *c*-axis oriented $(\text{Pb},\text{Ca})\text{TiO}_3$ thin films on MgO and SrTiO_3 substrates by the r.f. magnetron sputtering technique. Other authors have also reported on the production of $(\text{Pb},\text{Ca})\text{TiO}_3$ thin films, among them Maiwa et al.,¹² who reported on the preparation of $\text{Pb}_{0.7}\text{Ca}_{0.3}\text{TiO}_3$ thin films by a multiple-cathode r.f. magnetron sputtering method. In addition, Bao et al.¹³ prepared $(\text{Pb},\text{Ca})\text{TiO}_3$ thin films by a modified sol-gel technique, and other authors have also discussed the influence of calcium on the ferroelectricity of modified lead titanate on the form of the bulk.^{14,15}

This article reports on the production of calcium-modified lead titanate $[(\text{Pb},\text{Ca})\text{TiO}_3]$ thin films, which

form a solid solution between calcium titanate and lead titanate, by the polymeric precursor method.

2. Experimental

Lead (II) acetate trihydrate $(\text{Pb}(\text{CH}_3\text{COO})_2 \cdot 3\text{H}_2\text{O})$, calcium carbonate (CaCO_3) and Titanium (IV) isopropoxide $(\text{Ti}(\text{OCH}(\text{CH}_3)_2)_4$ were used as starting materials. Ethylene glycol and citric acid were used as polymerization/complexation agents for the process. Ammonium hydroxide was used to adjust the pH and to prevent lead citrate precipitation. Following the flow chart shown in Fig. 1, titanium citrates were formed by the dissolution of titanium IV isopropoxide in a water solution of citric acid (60–70°C). After homogenization of the Ti-citrate solution, a stoichiometric amount of $(\text{Pb}(\text{CH}_3\text{COO})_2 \cdot 3\text{H}_2\text{O})$ was dissolved in water and then added to the Ti-citrate solution while it was slowly stirred. Ammonium

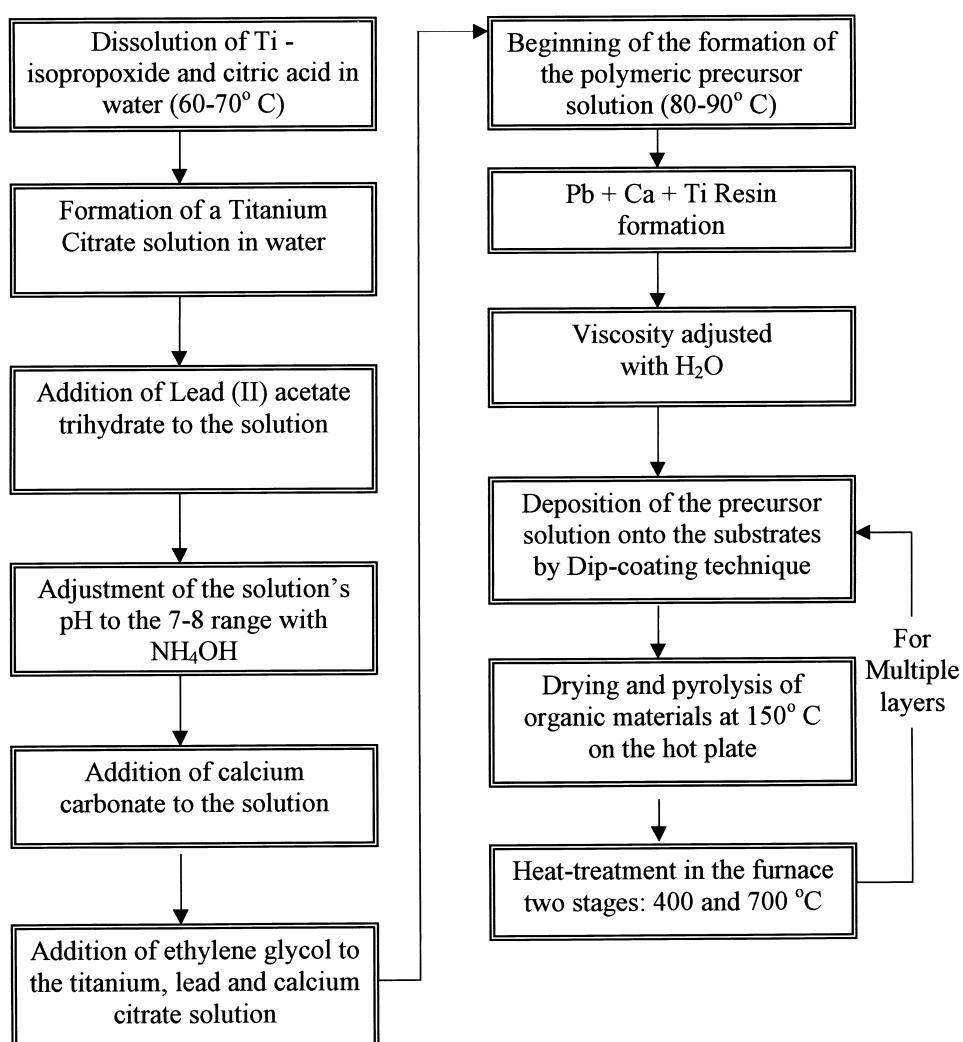


Fig. 1. Flow-chart illustrating the procedure for the preparation of $(\text{Pb}_{0.76}\text{Ca}_{0.24})\text{TiO}_3$ solution and film production.

hydroxide was added drop by drop until the pH reached 7–8. The complete dissolution of the salts resulted in a clear solution. Later, CaCO_3 was also slowly added, resulting in a clear solution. After homogenization of the solution containing Pb and Ca cations, ethylene glycol was added to promote mixed citrate polymerization by polyesterification reaction. The solution became more viscous with continued heating at 80–90°C, with no visible phase separation. The molar ratio among the lead–calcium and titanium cations was 1:1, the citric acid/metal molar ratio was fixed at 1.00, and the citric acid/ethylene glycol ratio was fixed at 60/40 (mass ratio). The viscosity of the deposition solution was adjusted to 15 mPas by controlling the water content. The thin films were prepared by a dipping platinum-coated silicon substrate in a PCT solution and subsequently pulling it up at a constant speed of 0.76 cm/min. After deposition, each layer was dried at 150°C on a hotplate for 20 min to remove residual solvents. The heat treatment was carried out in two stages: initial heating at 400°C for 2 h at a heating rate of 5°C/min to pyrolyze the organic materials, followed soon thereafter by heating to crystallize them. Each layer was pyrolyzed at 400°C and crystallized before the next layer was coated. This process was repeated several times to achieve the desired film thickness.

X-ray diffraction (XRD) patterns were obtained using a Cu K_α radiation source to determine the crystallinity of the films. The thickness of the coated film was measured by thin film cross-section analysis using scanning electron microscopy (SEM). Atomic force microscopy (AFM) was used to obtain an image reconstruction of

the sample's surface. These images allow accurate analyses to be made of the sample's surface and others parameters, such as roughness and grain size, to be quantified. A Digital Instruments Multi-Mode Nanoscope IIIa was used.

The ferroelectric properties of the $\text{Pb}_{0.76}\text{Ca}_{0.24}\text{TiO}_3$ thin film were evaluated using a capacitor structure of metal–ferroelectric–metal, on which the top Au (0.3 mm diameter) electrode was deposited by sputtering through a designed mask on to the film surfaces. A ferroelectric analysis was performed using the Radiant Technologies RT6000HVS ferroelectric test system. The capacitance–voltage (C – V) properties were characterized using Hewlett-Packard (4194A) impedance/gain phase analyzer, in which the capacitance value was measured using a small AC signal of 10 mV at 100 kHz. The dielectric constant and dissipation factor were measured as a function of frequency in a frequency range of 100 Hz to 10 MHz. The leakage current–voltage (I – V) characteristic was measured using a voltage source measurement unit (Keithley 237). All the measurements were taken at room temperature.

3. Results and discussion

3.1. Crystallographic structure

The crystallographic structure of the films was examined by the X-ray-diffraction technique (XRD). Fig. 2 illustrates the diffraction patterns of the film after heat

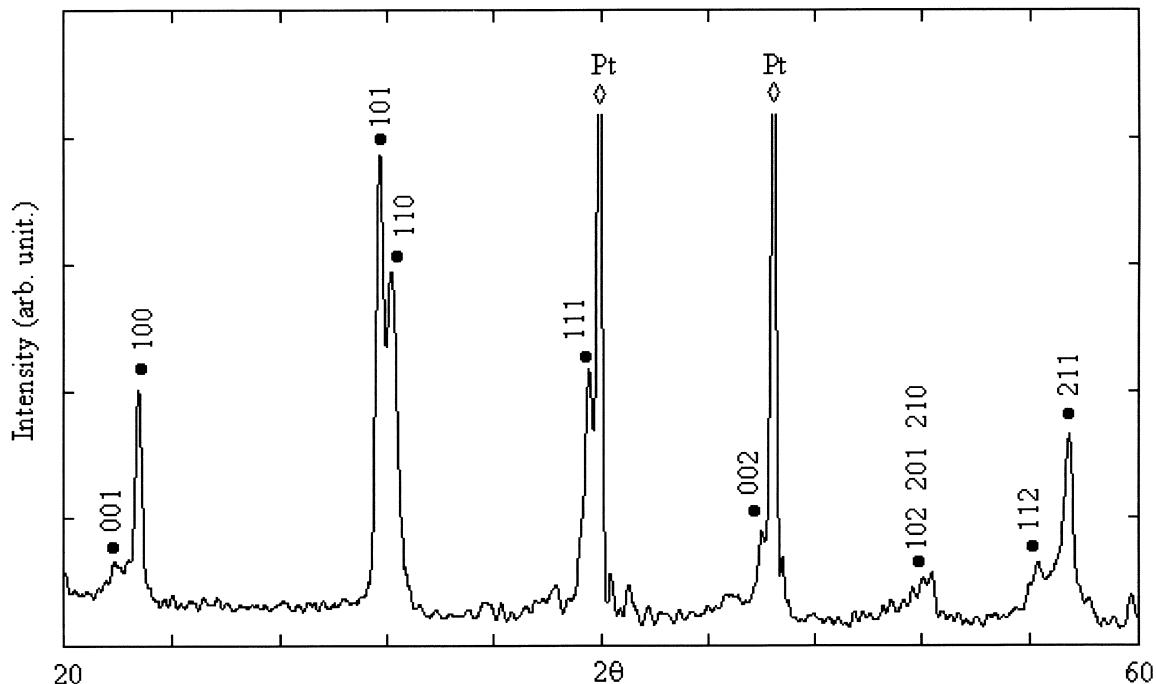


Fig. 2. X-ray diffraction patterns of $(\text{Pb}_{0.76}\text{Ca}_{0.24})\text{TiO}_3$ thin films on $\text{Pt}/\text{Ti}/\text{SiO}_2/\text{Si}$ substrate annealed at 700°C.

treatment at 700°C for 2 h. All the peaks are attributed to a tetragonal perovskite structure except those ascribed to the substrate (Pt peak). In addition, some of those peaks appear overlapped and a peak corresponding to the 111 diffraction line of Pt is observed. The XRD patterns also revealed that the films were polycrystalline, with no evidence of preferred orientation or secondary phases. The lattice parameters of the film and, therefore, the tetragonality of the film c/a , were obtained from the diffraction pattern. The typical tetragonality obtained for the PCT thin films is $c/a \sim 1.021$. The values reported here are similar to those reported by Martín et al.¹⁶

3.2. Surface morphology and microstructure

Scanning electron microscopy analysis showed the film thickness to be approximately 550 nm, and the film/substrate interface showed good adhesion (Fig. 3). AFM imaging was carried out in the contact mode, using a triangular shaped 200- μm long cantilever with a spring constant of 0.06 N/m. The scanning rate varied from 1 to 2 Hz and the applied force from 10 to 50 nN, depending on the sample/tip interactions. Surface roughness (rms) was calculated using the equipment's software routine.

The average grain size and surface roughness of the $\text{Pb}_{0.76}\text{Ca}_{0.24}\text{TiO}_3$ thin film were estimated using atomic force microscopy (AFM). Fig. 4 shows an image of a $\text{Pb}_{0.76}\text{Ca}_{0.24}\text{TiO}_3$ film annealed at 700°C for 2 h and characterized by a slight surface roughness with a uniform, crack-free, densely packed microstructure. On the other hand, PCT thin film with the same composition obtained by pulsed laser¹⁶ was characterized by the growth of isolated cubes and showed a porous morphology, which is useless for electrical applications.

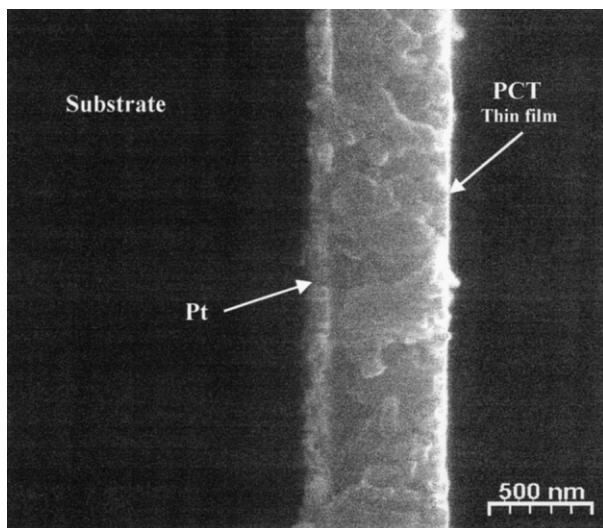


Fig. 3. Scanning electron micrographs of the cross-section of the PCT thin films deposited on Pt/Ti/SiO₂/Si substrate.

The average size and surface roughness of the spherical shaped grains obtained by the polymeric precursor method were close to 80 and 6.0 nm, respectively. This surface roughness is lower than that obtained by Martín et al.,¹⁶ who reported roughnesses of 30–40 nm for PCT films with the same $x=0.24$ composition on Pt/Ti/SiO₂/Si produced by the laser ablation technique.

3.3. Ferroelectric and dielectric properties

A 550-nm-thick film was used for the electrical and ferroelectric measurements. Fig. 5 illustrates the variation of the dielectric constant and the dissipation factor ($\tan \delta$) as a function of frequency in the range of 100 Hz–10 MHz for films deposited on Pt/Ti/SiO₂/Si substrates. The dielectric properties of different dot electrodes of the films changed by 2–3%, confirming the homogeneous

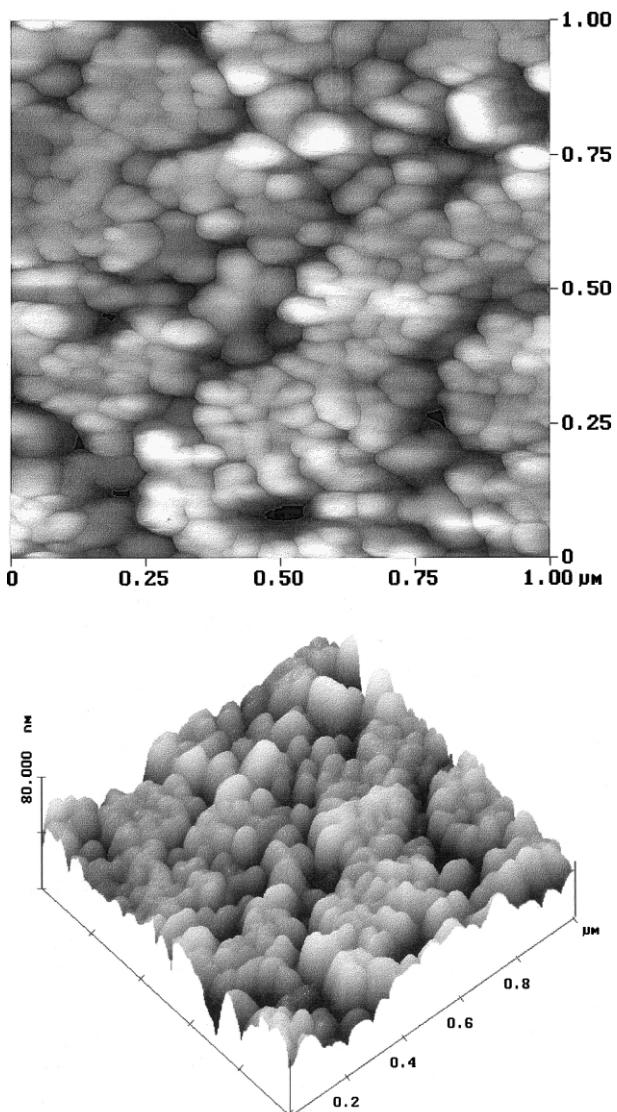


Fig. 4. Atomic force microscopic surface image of a PCT thin film obtained by the polymeric precursor method and annealed at 700°C.

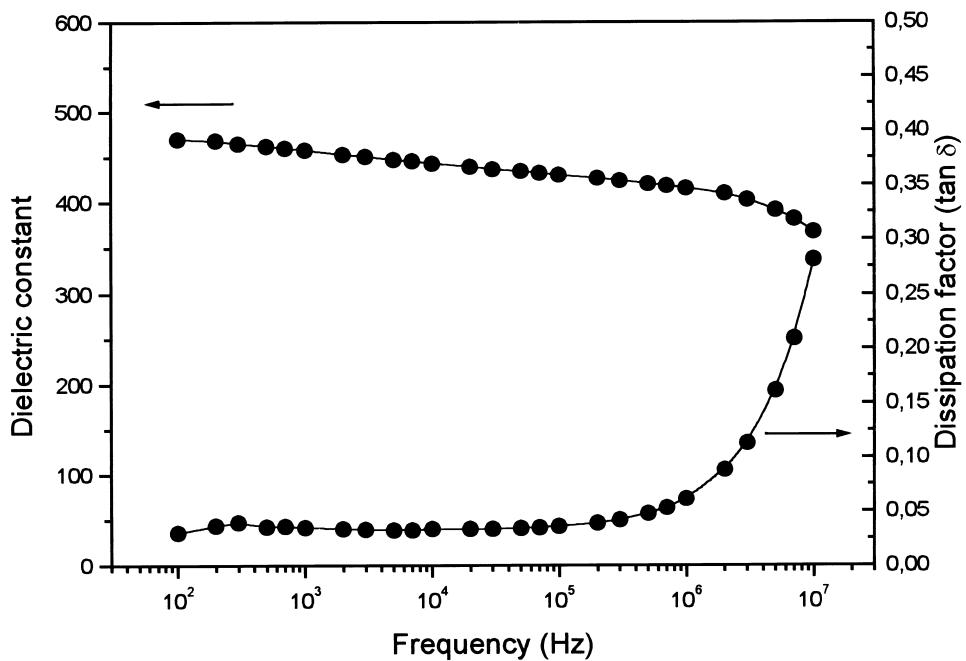


Fig. 5. Frequency dependence of dielectric constant and dissipation factor of PCT thin film capacitor on Pt/Ti/SiO₂/Si.

composition and uniform thickness of PCT thin films prepared by the polymeric precursor method. The dielectric constant and the dissipation factor ($\tan \delta$) at a frequency of 1 kHz were 457 and 0.03, respectively. This film showed little dispersion dielectric constant, displaying a decline of approximately 20% when the applied frequency increased from 100 Hz to 10 MHz. The rapid increase of the dissipation factor at a frequency above 10⁶ Hz may be related to space charge conductivity effects. Similar dielectric constant and dissipation factors versus frequency behaviours have been reported in other thin films.^{17–19} These values exceed several of the values reported for PCT thin films with similar compositions prepared by other techniques, as summarized in Table 1.

Fig. 6 displays the typical C - V curve for MFM capacitors. Capacitance dependence on the voltage is strongly nonlinear, confirming the ferroelectric properties of the film. The two peaks which characterize spontaneous polarization switching are clearly shown in

Fig. 6. Also, the C - V curve displays a symmetry in the maximum capacitance values that can be observed in the vicinity of the spontaneous polarization switch. However, the centre of the C - V curves was not located in the zero bias field, but shifted toward the positive bias field, to about +0.4 V. In addition, PCT thin films obtained by the modified sol-gel¹³ technique show asymmetries in the maximum capacitance values observed in the vicinity of the spontaneous polarization switching of C - V curves, as well as a shift of the C - V curves of approximately 2 V toward the positive bias field.

The ferroelectric properties of the PCT film were confirmed by hysteretic measurements. Fig. 7 shows the P - E curve of the $Pb_{0.76}Ca_{0.24}TiO₃$ thin films. In addition, a small displacement of the hysteretic loop was also observed in the PCT thin film, which is in agreement with that of the C - V curve measurements. As shown in Fig. 7, the remanent polarization (P_r) and the coercive field (E_c) were 17 μ C/cm² and 75 kV/cm, respectively. A high value of remanent polarization is essential for applications such as non volatile memories. The values obtained in this study were higher than those reported in the literature,²⁰ for the same composition. Table 2 shows the ferroelectric properties of the PCT thin films prepared by the polymeric precursor method compared with several values reported for PCT with close compositions for thin films prepared by other techniques.

Fig. 8 shows the measured current density (J) versus the applied voltage (V) in a $\log(J)$ vs $\log(V)$ plot for the $Pb_{0.76}Ca_{0.24}TiO₃$ film. The voltage is applied in 0.2 V steps and the current is measured after a delay time of 1 s for each voltage. Two clearly different regions can be

Table 1
Electrical properties of PCT films according to the literature

| Processing temp. (°C) | Dielectric constant (1 kHz) | $\tan \delta$ (1 kHz) | Thickness (nm) | Deposition method |
|-----------------------|-----------------------------|-----------------------|----------------|-------------------|
| 650 | 171 ($x=0.30$) | 0.027 | 1000 | Sol-gel |
| 650 | 187 ($x=0.20$) | 0.022 | 1000 | Sol-gel |
| 800 | 330 ($x=0.10$) | 0.032 | 1000 | Sol-gel |
| 650 | 116 ($x=0.24$) | – | 500 | Sol-gel |
| 650 | 42 ($x=0.24$) | – | 500 | Sol-gel |
| 650 | 230 ($x=0.24$) | 0.027 | 500 | Modified sol-gel |
| 700 | 365 ($x=0.30$) | – | 300 | Sol-gel |
| 700 | 457 ($x=0.24$) | 0.030 | 550 | This study |

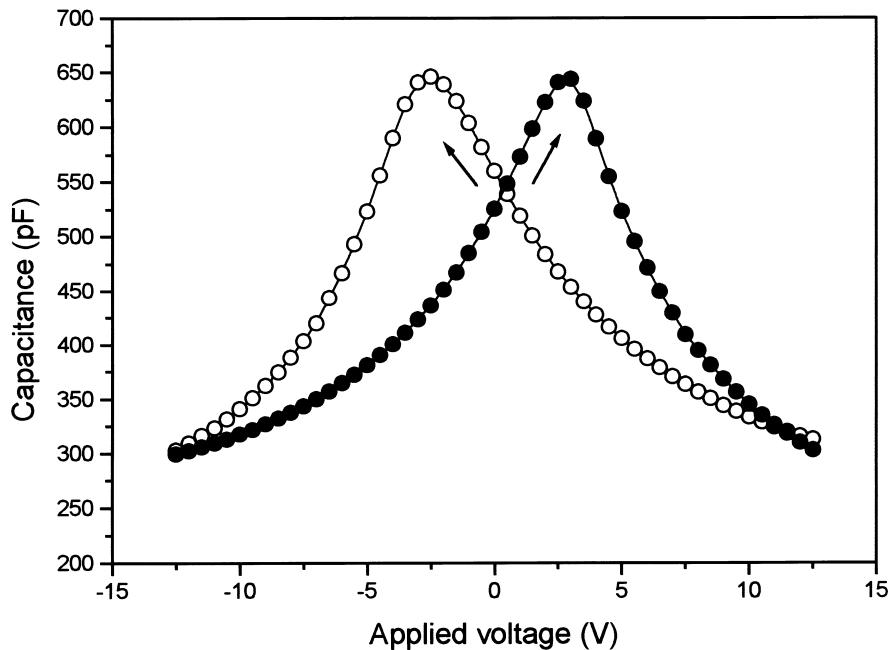


Fig. 6. Dependence of the capacitance of the PCT thin film on d.c. bias voltage.

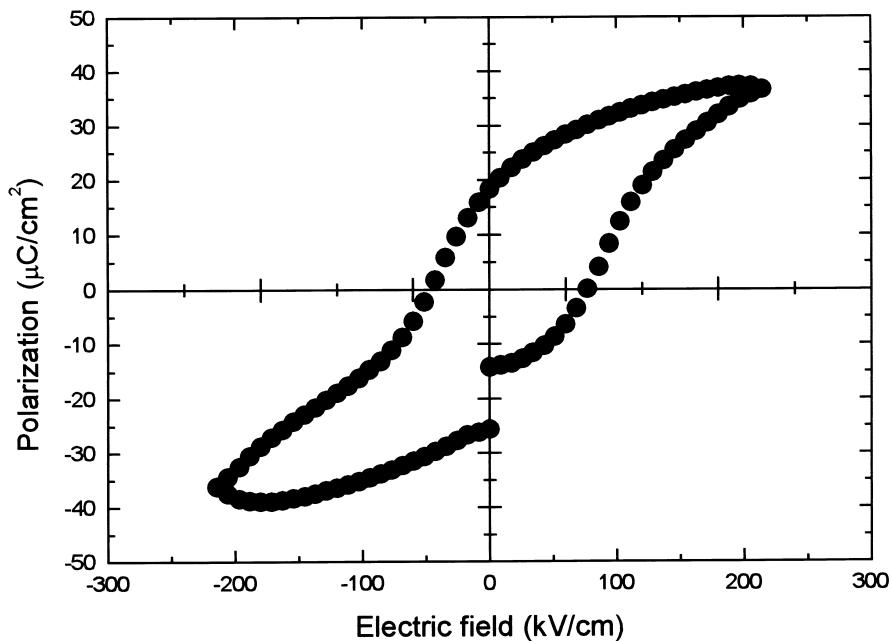


Fig. 7. A typical hysteresis loop of a PCT thin film on a Pt/Ti/SiO₂/Si substrate obtained by the polymeric precursor method.

seen, i.e. one in the low voltage region below 6 V, where the current density is almost proportional to the applied voltage, and another in the high voltage region above 6 V, which increases exponentially with the applied voltage. In the low field region, the $\log(J)$ vs $\log(V)$ curve has slope of ~ 1 , indicating that the current in the low field region is ohmic-like. The $\log(J)$ vs $\log(V)$ curve in the high field region has a slope of ~ 10 . The leakage

current in the high field has been postulated to be due to Schottky or Poole-Frenkel emission. The leakage current levels of the $\text{Pb}_{0.76}\text{Ca}_{0.24}\text{TiO}_3$ film obtained by the polymeric precursor method are in the range of $10^{-8}\text{--}10^{-7}\text{ A/cm}^2$ at 2.0 V. The breakdown voltage, defined as the bias voltage at which the leakage current density reaches 10^{-3} A/cm^2 through the capacitor, was found to exceed 200 kV/cm.

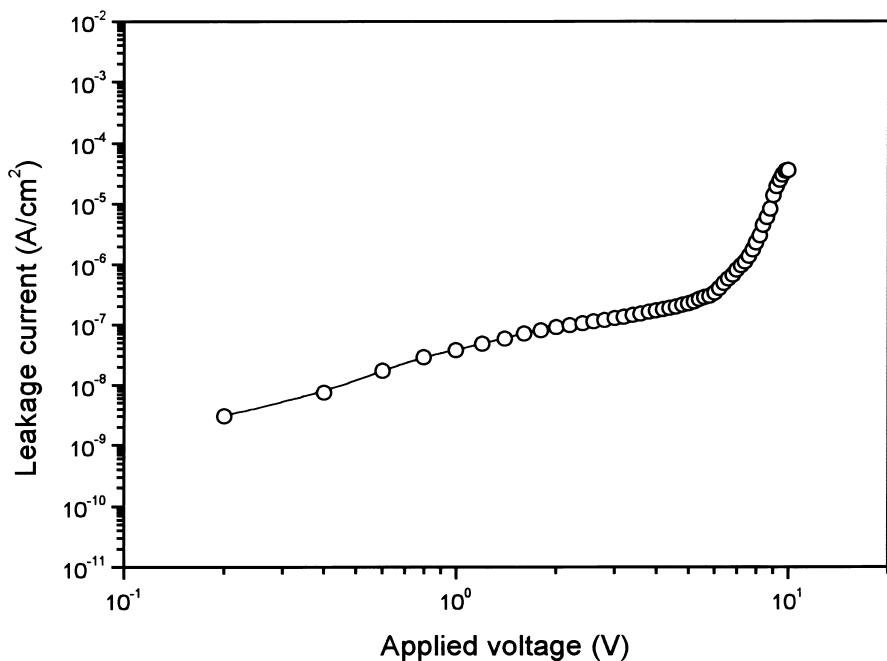


Fig. 8. Leakage current characteristics with the applied voltage of a PCT thin film capacitor on Pt/Ti/SiO₂/Si.

Table 2
Ferroelectrical properties of PCT films according to the literature

| Processing temp. (°C) | Remanent polarization P_r ($\mu\text{C}/\text{cm}^2$) | Coercive field E_c (kV/cm) | Thickness (nm) | Deposition method |
|-----------------------|---|------------------------------|----------------|-------------------|
| 600 | 15 ($x=0.24$) | 64 | 500 | Modified-Sol-gel |
| 800 | 15 ($x=0.10$) | 70 | 1000 | Sol-gel |
| 700 | 15 ($x=0.15$) | 117 | 300 | Sol-gel |
| 650 | 4.6 ($x=0.30$) | 68 | 1000 | Sol-gel |
| 650 | 8.0 ($x=0.20$) | 64 | 1000 | Sol-gel |
| 650 | 6.0 ($x=0.24$) | 100 | 700 | Sol-gel |
| 650 | 9.0 ($x=0.25$) | 77 | 500 | Sol-gel |
| 550 | 0.55 ($x=0.24$) | 139 | 500 | Pulsed laser |
| 550 | 1.50 ($x=0.24$) | — | 600 | Laser ablation |
| 700 | 17 ($x=0.24$) | 75 | 550 | This study |

4. Conclusions

We have demonstrated, for the first time, the growth of ferroelectric $\text{Pb}_{0.76}\text{Ca}_{0.24}\text{TiO}_3$ thin films directly on Pt(111)/Ti/SiO₂/Si(100) substrates by the polymeric precursor method, using the dip-coating technique and heat treatment at 700°C in air. The quality of films obtained by this simple technique is comparable to that obtained through other techniques. Polycrystalline, homogenous, crack-free $\text{Pb}_{0.76}\text{Ca}_{0.24}\text{TiO}_3$ thin films were prepared. A smooth, dense surface was observed by AFM, which also revealed low surface roughness (6.0 nm) in multilayer films. XRD results showed a tetragonally structured polycrystalline film with a c/a ratio of ~ 1.021 . The multilayer thin films consisted of grains of approximately 80 nm having a film thickness of 550 nm.

Dielectric properties were measured for the MFM configuration. The PCT thin films showed ferroelectric behaviour with a dielectric constant of 457 and a loss tangent of 0.03 at 1 kHz. The C - V characteristics of the MFM structure showed a typical butterfly loop, confirming the ferroelectric properties of the film, which are related to ferroelectric domain switching. The films showed a remanent polarization of $P_r = 17 \mu\text{C}/\text{cm}^2$ and a coercive field of $E_c = 75 \text{ kV}/\text{cm}$. I - V measurements displayed an ohmic behavior at low voltage (< 6 V) with a possible Schottky (SK) or Poole–Frenkel (PF) mechanism at high voltages (> 6 V). The leakage current of the PCT thin film was in the order of 10^{-8} – $10^{-7} \text{ A}/\text{cm}^2$ at 2 V. These results suggest that the polymeric precursor method is suitable to produce calcium-modified lead titanate ($\text{Pb},\text{Ca}\text{TiO}_3$) thin films with good ferroelectric properties.

Acknowledgements

The authors gratefully acknowledge the financial support of the Brazilian financing agencies FAPESP, CNPq, PRONEX/FINEP and CAPES.

References

1. Paz de Araujo, C. A., Cuchlaro, J. D., McMillan, L. D., Scott, M. C. and Scott, J. F., Fatigue-free ferroelectric capacitors with platinum electrodes. *Nature*, 1995, **374**, 672.
2. Lu, C.-H. and Wen, C.-Y, New non-fatigue ferroelectric thin films of barium bismuth tantalite. *Mater. Lett.*, 1999, **38**, 278.

3. Kumazawa, H. and Masuda, K., Fabrication of barium titanate thin films with a high dielectric constant by a sol-gel technique. *Thin Solid Films*, 1999, **353**, 144.
4. Brazier, M., Mansour, S. and McElfresh, M., Ferroelectric fatigue of $\text{Pb}(\text{Zr},\text{Ti})\text{O}_3$ thin films measured in atmospheres of varying oxygen concentration. *Appl. Phys. Lett.*, 1999, **74**(26), 4032.
5. Li, A., Ge, C., Lü, P., Wu, D., Xiong, S. and Ming, N., Growth and ferroelectric properties of sol-gel derived $(\text{PbLa})\text{TiO}_3$ films on metallic LaNiO_3 -coated substrates. *Mater. Lett.*, 1997, **31**, 15.
6. Miura, K. and Tanaka, M., Effect of La-doping on fatigue in ferroelectric perovskite oxides. *Jpn. J. Phys.*, 1996, **35**(6A), 3488.
7. Pontes, F. M., Leite, E. R., Longo, E., Varela, J. A., Araujo, E. B. and Eiras, J. A., Effects of the postannealing atmosphere on the dielectric properties of $(\text{Ba},\text{Sr})\text{TiO}_3$ capacitors: Evidence of an interfacial space charge layer. *Appl. Phys. Lett.*, 2000, **76**(17), 2433.
8. Pontes, F. M., Longo, E., Rangel, J. H., Bernardi, M. I., Leite, E. R. and Varela, J. A., $\text{Ba}_{1-x}\text{Sr}_x\text{TiO}_3$ thin films by polymeric precursor method. *Mater. Lett.*, 2000, **43**, 249.
9. Pontes, F. M., Rangel, J. H. G., Leite, E. R., Longo, E., Varela, J. A., Araujo, E. B. and Eiras, J. A., Low temperature synthesis and electrical properties of PbTiO_3 thin films prepared by the polymeric precursor method. *Thin Solid Films*, 2000, **366**, 232.
10. Zanetti, S. M., Longo, E., Varela, J. A. and Leite, E. R., Microstructure and phase evolution of SrTiO_3 thin films on Si prepared by the use polymeric precursor. *Mater. Lett.*, 1997, **31**, 173.
11. Yamaka, E., Watanabe, H., Kimura, H., Kanaya, H. and Ohkuma, H., Structural, ferroelectric, and pyroelectric properties of highly c-axis oriented $\text{Pb}_{1-x}\text{Ca}_x\text{TiO}_3$ thin films grown by radio-frequency magnetron sputtering. *J. Vac. Sci. Technol. A*, 1988, **6**(5), 2921.
12. Maiwa, H. and Ichinose, N., Preparation and properties of $(\text{Pb},\text{Ca})\text{TiO}_3$ thin films by multiple-cathode sputtering. *Jpn. J. Appl. Phys.*, 1997, **36**(9B), 5825.
13. Bao, D., Wu, X., Zhang, L. and Yao, X., Preparation, electrical and optical properties of $(\text{Pb},\text{Ca})\text{TiO}_3$ thin films using a modified sol-gel technique. *Thin Solid Films*, 1999, **350**, 30.
14. Mendiola, J., Alemany, C., Pardo, L. and Gonzalez, A., Poling reversal effects on piezoelectricity of calcium modified lead titanate ceramic. *Ferroelectrics*, 1989, **94**, 209.
15. Mendiola, J., Jiménez, B., Alemany, C., Pardo, L. and Del Olmo, L., Influence of calcium on the ferroelectricity of modified lead titanate ceramics. *Ferroelectrics*, 1989, **94**, 183.
16. Martín, M. J., Mendiola, J. and Zaldo, C., Influence of deposition parameters and substrate on the quality of pulsed-laser-deposited $\text{Pb}_{1-x}\text{Ca}_x\text{TiO}_3$ ferroelectric films. *J. Am. Ceram. Soc.*, 1998, **81**(10), 2542.
17. Mafei, N. and Krupanidhi, S. B., Electrical characteristics of excimer laser ablated Bismuth titanates films on silicon. *J. Appl. Phys.*, 1992, **72**, 3617.
18. Joshi, P. C. and Krupanidh, S. B., Structural and electrical studies on rapid thermally processed ferroelectric $\text{Bi}_4\text{Ti}_3\text{O}_{12}$ thin films by metalloorganic solution deposition. *J. Appl. Phys.*, 1992, **72**(12), 5817.
19. Sedlar, M. and Sayer, M., Structural and electrical properties of ferroelectric bismuth titanate thin films prepared by the sol gel method. *Ceram. International*, 1996, **22**, 241.
20. Sirera, R., Calzada, M. L., Carmona, F. and Jiménez, B., Ferroelectric thin films of calcium modified lead titanate by sol-gel processing. *J. Mater. Sci. Lett.*, 1994, **13**, 1804.